Invited Paper

New approaches towards the understanding of the catastrophic optical damage process in in-plane diode lasers

Jens W. Tomm*[a], Mathias Ziegler[a], Vadim Talalaev[a], Clemens Matthiesen[a], Thomas Elsaesser[a], Marwan Bou Sanayeh[b], Peter Brick[b], Martin Reufer[b]
[a]Max-Born-Institut, Max-Born-Str. 2 A, 12489 Berlin, Germany
[b]OSRAM Opto Semiconductors GmbH, Leibnizstr. 4, 93055 Regensburg, Germany

ABSTRACT

The microscopic processes accompanying the catastrophic optical damage process in semiconductor lasers are discussed. For 808 and 650 nm edge-emitting broad-area devices relevant parameters such as surface recombination velocities, bulk and front facet temperatures are determined and discussed. Facet temperatures vs. laser output and temperature profiles across laser stripes reveal a strong correlation to near-field intensity and degradation signatures. Furthermore, the dynamics of the fast catastrophic optical damage process is analyzed by simultaneous high-speed infrared thermal and optical imaging of the emitter stripe. The process is revealed as fast and spatially confined. It is connected with a pronounced impulsive temperature flash detected by a thermocamera.

Keywords: catastrophic optical damage, 808 and 650 nm broad-area devices, facet temperature

1. INTRODUCTION

The optical feedback in edge-emitting semiconductor diode lasers originates from the partial reflection of the generated light at the front and rear facet. Fundamental mode lasers were the first type of diode lasers, where the facet loads reached levels at which facet degradation became a cardinal bottleneck for device reliability. A main degradation mode has been called 'catastrophic optical damage' (COD). It involves distinct physical destruction of a facet, in most cases the front facet. After its initialization at certain levels of optical and thermal load, called 'COD threshold', it appears as a very fast explosion-like process. Since the beginning of the 1990s a lot of effort has been put into understanding the underlying mechanisms and developing technological measures to increase the COD threshold. Sophisticated methods such as the E2 technology have been developed for facet passivation and coating.[1-2] For the time being the COD-problem as major degradation source has been solved, and single mode lasers with emission powers of several 100 mW are commercially available. Multimode broad-area (BA) lasers underwent a vast development as well, and even monolithic arrays with widths of one cm and fill factors of 20-50 percent have been realized on this basis. The facet loads in these devices which were named 'cm-bars' reached the order of 10 mW/µm. Recently, however, such cm-bars approached the kW level and the facet loads in these multimode devices exceed now 120 mW/µm.[3] As such, degradation effects (including the COD) that originate from the facets are gaining relevance for this class of multimode devices. The adaptation of existing facet technologies to cm-bars and the ongoing trend towards even higher facet loads require a deeper understanding of the microscopic mechanisms of gradual facet degradation and the subsequent (fast) COD process.

In this paper we report on measurements that provide some more insight into the physics of the COD process in 808 and 650 nm emitting BA lasers. These devices are considered here as representative segment out of a cm-bar array. First we give a brief overview on the state of research on the COD process. The important role that surface recombination plays will be high-lighted. We present experiments that help to quantify the surface recombination at device facets. For the same devices, we report on facet temperature measurements based on micro Raman (µR) spectroscopy. These data show the impact of surface recombination on the facet temperature. The direct monitoring of the fast COD process, however, requires a faster probe than the µR technique. Thus the dynamics of the COD process are analyzed by simultaneous high-speed optical and infrared thermal imaging (TI) of the active region at the front facet. The COD process is revealed as fast (<2.3 ms) and spatially confined ($< 8.8 \times 8.8\ \mu m^2$). It is connected with a pronounced impulsive temperature flash detected by TI.

*tomm@mbi-berlin.de; phone 49 30 63921453; fax 49 30 63921453; www.mbi-berlin.de

Novel In-Plane Semiconductor Lasers VIII, edited by Alexey A. Belyanin, Peter M. Smowton,
Proc. of SPIE Vol. 7230, 72300V · © 2009 SPIE · CCC code: 0277-786X/09/$18 · doi: 10.1117/12.806701

2. THE CATASTROPHIC OPTICAL DAMAGE PROCESS

The COD process is commonly explained by a thermal runaway process.[4-6] Re-absorption of laser light leads to strong local heating, eventually reaching a critical temperature level where the feedback loop of thermally induced band gap shrinkage and re-absorption enhancement cannot be balanced anymore by the materials' thermal conductance.[7] As a result, the semiconductor, in particular the quantum well (QW) layer, start melting locally.[4,8] This melting front propagates along the resonator as long as enough heat is provided by further absorption of laser light. After successive re-crystallization a network of defects is left behind, which leads to a vastly enhanced non-radiative recombination rate, eventually shifting the lasing threshold to higher values or even makes lasing impossible at all. Thus the device cannot be used anymore. The damage typically manifests itself as dark regions in the electroluminescence pattern.

The spatial extension of the resulting defect region is found to be confined in vertical direction to the QW and part of the waveguide to approximately 50-200 nm.[8-12] In lateral directions, the determined widths vary widely between values on the order of 1-10 µm at the front facet.[8,10,12,13] While this region is extending along the resonator - up to a high fraction of its total length - a spreading into many branches is possible, reaching lateral extensions of up to a high fraction of the total stripe width, i.e., of many 10 µm for high-power BA lasers.[8][10]

The explanation for this behavior is related to the pumping geometry and the composition of the materials involved. The optical pumping is extended along the lateral dimension to the stripe width, modulated by filamentation and can be characterized by measuring the optical near-field. In the vertical dimension the optical mode profile determines the amount of optical facet load extending not significantly further than the waveguide. In the case of GaAs-based lasers, barrier layers such as the waveguide and cladding usually contain a high mol-fraction of Al. Hence the melting point of these layers is much higher than that of the QW materials, e.g., for GaAs it is ~ 1500 K whereas for AlAs it is ~ 2000 K.[14] Consequently, it is more likely for the QW to melt before the surrounding materials reach their melting points. It is also possible that a change in the III-V stoichiometry (e.g., by diffusion of group-V atoms out of the lattice) may occur at considerably lower temperatures of a few 100 °C.[9,15] However, not all aspects of the microscopic processes have been uncovered yet, partly because of a lack of sufficient spatio-temporally resolved studies. That renders one of the motivations for our work.

Different paths towards COD are known; it can be induced e.g., by operating the laser diode for a longer time at a high injection level or by increasing the injection current straight beyond the COD threshold. The destructive process however, shows always the same or at least very similar characteristics. The difference between both paths lies mainly in how the laser diodes reach their critical temperature at the front facet. Three main processes can be identified that lead to the detrimental facet heating:

(i) Non-radiative recombination of carriers from re-absorption (e.g., interband absorption) of laser light at the front facet or optical absorption at non-semiconductor materials, i.e., at the facet coating or at oxides and pollutants. We call this process 're-absorption heating'.

(ii) Non-radiative recombination of carriers at surface states injected from the pn-junction. This process represents a heating process directly caused by surface-recombination.

(iii) Heating of the bulk materials is always an additional contribution to the final temperature at the front facet. We will show that although this process does not contribute to the facet overheating (with respect to the bulk temperature), it takes an important part in the COD process.

The *surface recombination*, see (ii), promotes extra facet heating at all levels of electrical pumping and below the lasing threshold it is probably the major mechanism contributing to the facet overheating. Therefore it is likely to contribute to the gradual mechanisms, which lower the COD threshold before the onset of the (fast) COD process. Thus the surface recombination at the active region of a device requires special attention when understanding of the whole process towards the COD is desired.

The two heating mechanisms based on recombination, (i) and (ii), are obviously subject to the quality of the facet. If the quality is poor, e.g., if it contains a high density of surface states, facet heating increases. It is known that operation of the device leads to alteration of the facet or even the top region of the bulk material near the surface, thereby experiencing chemical processes such as oxidation, which is responsible for an enhancement of the defect density or of the absorption strength.[15-20]

3. SURFACE RECOMBINATION MEASUREMENTS

The spatial distribution of non-equilibrium carriers in a semiconductor is well described by rate equations. The parameter *surface recombination velocity* s_v is a proportionality factor introduced into the boundary condition describing the drain for carriers at a surface.[21] This phenomenological parameter (with the units of a velocity, namely cm/s) is also used to describe the situation at the front facet of a diode laser. Its measurement, however, is difficult and relies in most approaches on experiments, which monitor the spatial distribution of non-equilibrium carriers. The extraction of s_v is subsequently accomplished via analysis of the rate equations. The experimental difficulties become even more substantial when the active region of a diode laser, i.e., the tiny aperture at the facet of a BA laser where the laser light emerges, should be considered.

In an earlier study, we reported on s_v-measurements of laser structures.[22] Nanoscopic steady-state photoluminescence (PL) measurements carried out with a near-field optical scanning microscope in concert with conventional time-resolved (TR) PL measurements (determination of the non-equilibrium carrier lifetime τ) allowed independent analysis of s_v and the in-plane diffusion constant D in the region of interest, namely at the location, where the front facet intersects the QW plane. The drawback of this approach is that it can not be applied to regular devices. Test samples with unmetallized p-side are required, preferably from the same processing batch (same wafer, same treatment). Moreover, the experimental effort is too complex to be implemented into an industrial environment.

A simplified and straightforward approach for s_v-measurements for given devices relies on two color TR PL measurements at the front facet in the range of the *substrate*.[23] Although now the measurement is not made directly at the active region, a material is analyzed, which experienced exactly the same technological treatment. Carrier transients are derived for two different excitation wavelengths, namely λ_{ex} = 790 and 395 nm. For λ_{ex}=790 nm, the penetration depth is in the range of microns (absorption coefficient $\alpha \sim 1.2\times10^4$ cm^{-1}) and, thus, PL originates mainly from the bulk of the devices, whereas the PL from the topmost surface layer is detected with excitation at λ_{ex} =395 nm, where $\alpha \sim 3\times10^5$ cm^{-1}. Analysis of the PL-transient *ratios*, see Fig. 1 (right), allows for the determination of s_v, while eliminating the influence of the bulk lifetime. The setup is based on a mode-locked Ti:sapphire laser (pulse duration <100 fs, repetition rate 82 MHz, average excitation power ~10 mW) as the excitation source and a streak camera for TR-PL detection.[24] In Fig. 1 we show data from two devices, A and B, from a batch of 808 nm emitting devices with a standard facet coating. While standard electrical and optical parameters such as threshold and efficiency are identical for both devices, the only distinction between the two devices is the facet process. The two applied processes are called here A and B and we use the same denotations for the devices representing the batch specific behavior.

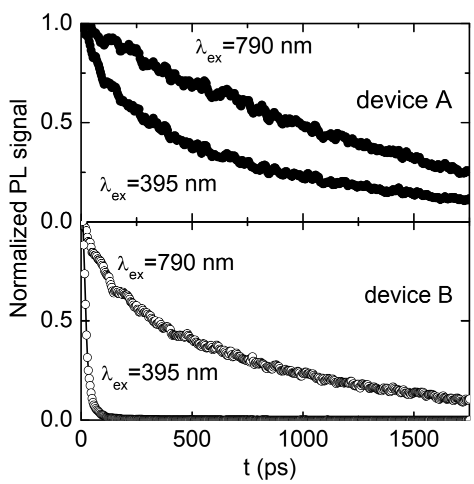

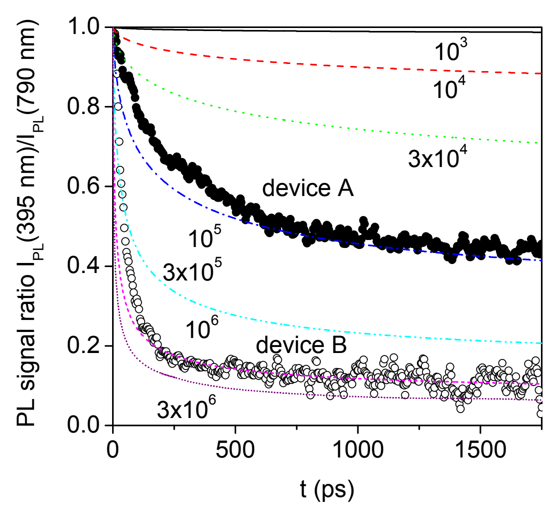

Fig. 1. (Left) Original PL transients for devices A (solid symbols) and B (open symbols). The spectrally integrated and normalized PL intensity is plotted as a function of time. (Right) Ratios of PL intensities measured for device A and B as a function of time. The fan chart of lines is calculated with the parameter $s_v=10^3 \ldots 3\times10^6$ cm/s from top to bottom.

Thus the facet process is here the parameter that allows for controlling the density of surface recombination centers and, eventually, for tailoring s_v. Figure 1 shows clearly that the s_v-values estimated for device B exceed the one we got for device A by almost an order of magnitude. The calculations that allow estimating s_v-values, see fan chart in Fig. 1, are based on the work of Ahrenkiel.[25,26]

Since most COD scenarios consider s_v a parameter that substantially influences device degradation and initializes the COD process, it is of interest to investigate how exactly this parameter contributes to the actual facet overheating. Facet temperatures are measured using µR technique with a Dilor x-y- spectrometer. Temperatures are derived from both the spectral shifts and the intensity ratios of Stokes and anti-Stokes phonon lines with an accuracy of ~ 10 K. The 488 nm line of an Ar-ion laser serves for excitation (excitation power ~850 µW, spot diameter $Ø_{1/e}$ ~1 µm) of the front facets in the range of the active region. The heat-sink temperature was 25 °C.

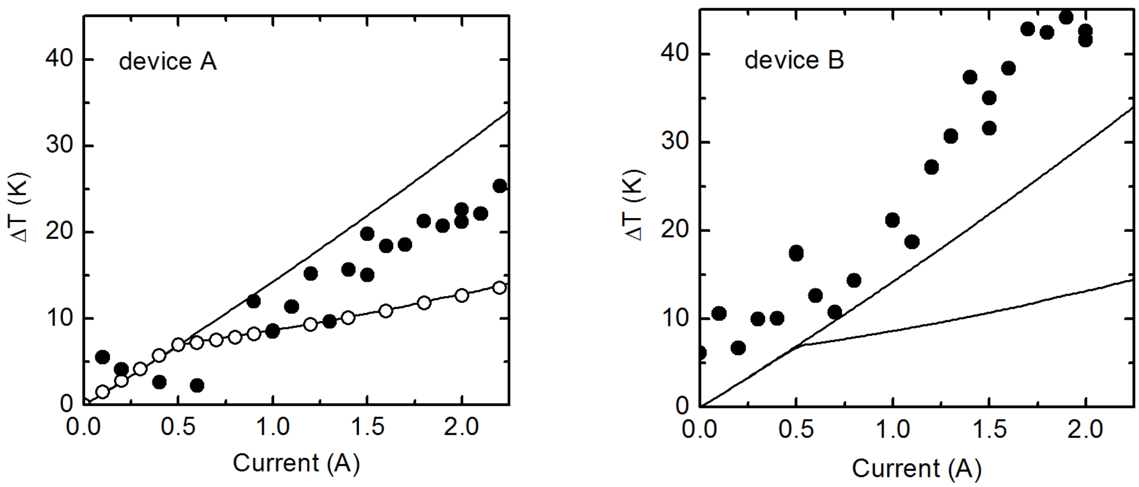

Fig. 2. Temperature increases above the heat-sink temperature of 25°C for devices A and B. Bulk temperature increases are given by the full lines which are $\Delta T_{bulk}=(U\times I-P_{opt})R_{th}$, and the dotted lines are $\Delta T=U\times I\times R_{th}$ as upper limit for the bulk temperature of non-lasing devices. The thermal resistance (R_{th}=7.5 K/W) is derived from bulk temperature data which are independently obtained by TI for device A; see open circles. Facet temperatures are marked by full circles.

Experimentally determined temperatures of the active region within the bulk and at the facet for devices A and B are presented in Figs. 2 (left) and (right), respectively. The temperature increase ΔT relative to the heat-sink temperature is plotted as a function of the injection current. Full circles stand for facet temperatures.

When confining the analysis of the µR data to the range *below the laser thresholds*, we find average values ΔT=(4.0±1.5)°C and ΔT=(11±4)°C for device A and B, respectively. Since the bulk temperatures in both devices are almost equal, the different facet temperatures confirm the thesis that below the laser threshold surface recombination represents a major source of facet heating.

In the *above-threshold range*, we find the bulk temperatures of devices A and B, as expected, to be also almost the same. The facet temperatures, however, are strikingly different. Device A displays a moderate increase of facet temperature with current, exceeding the bulk temperature by at most 10 K in the current range shown. For device B this increase amounts to 30 K and the rate of increase changes noticeably at the threshold. Such a change is interpreted as a change of the dominant facet heating mechanism. This change is very likely to originate from surface recombination to re-absorption as dominating heating mechanism. This reveals that an increased surface recombination velocity (heating via electrically injected carriers) is accompanied by increased re-absorption (heating via photo-excited carriers). In principle, the microscopic nature of defects that give rise to enhanced surface recombination on the one hand and re-absorption heating on the other hand could be different but – should there be such a distinction – than both types will originate from the different facet preparations applied. In any case, increased facet temperatures accelerate device degradation in both the *slow* gradual degradation mode (defect accumulation during regular operation), and the *fast* COD mode (thermal runaway initialized by reaching a critical facet temperature).

4. REAL-TIME IMAGING OF THE COD PROCESS

After having discussed the importance of surface recombination and its parameter s_v as initializing heat source for gradual degradation and COD, we proceed to the (fast) COD process itself. We will discuss results obtained on red-emitting BA lasers, which serve as model devices here.

The setup for real-time COD imaging has been described by Ziegler et al. [27] A coated Si-filter is tilted and used as dichroic mirror that transmits thermal IR radiation (used in the range 3.4 µm<λ<6 µm) and reflects incident laser light. This reflected light is imaged by a conventional Si-CCD camera (spectral range: 300-1100 nm), with a microscopic objective lens. It contains information about the spatial distribution of the laser-light intensity at the front facet, i.e., the optical nearfield (NF). The TI-system records 64×40 pixel images (spatial resolution 8.8 µm/pixel) at a frequency of ~430 Hz. Thus the whole laser device and about 200 µm of the submount are imaged. The parameters where chosen as a compromise between high temporal resolution, high thermal contrast and high probability of catching the COD event. First it should be noted that, since the COD event is singular, only a free-run recording (i.e., no sampling) is possible. Second, since the COD event is very short, a high filling fraction for the image recording is necessary, i.e., a high ratio of integration time versus dead time. The dead time is composed of the CCD-read-out time and other electronic offsets and as such essentially depends on the number of CCD pixels (divided in discrete blocks) used in the measurement. Therefore the optimized image barely contains the entire laser chip. The resulting block size resulted in a dead time of 0.3 ms. An integration time of 2 ms was chosen to give both a high thermal contrast (20 mK) and a high probability of recording the COD event. Consequently, the temporal resolution is restricted to 2.3 ms. The injection current was ramped with a frequency of 0.5 Hz from zero to above the COD level in discrete steps of 20 mA. Information on the laser bulk temperature towards COD is obtained by imaging the front facet with the thermographic camera. Figure 3 show thermal images around the occurrence of a COD event, taken out from a series of 1.2×10^5 images. Using an earlier calibration measurement the temperature increases of the region where COD occurred (COD seed, red line) and of the entire 100 µm wide active stripe (black line) are plotted as functions of injection current in Fig. 3 (e).

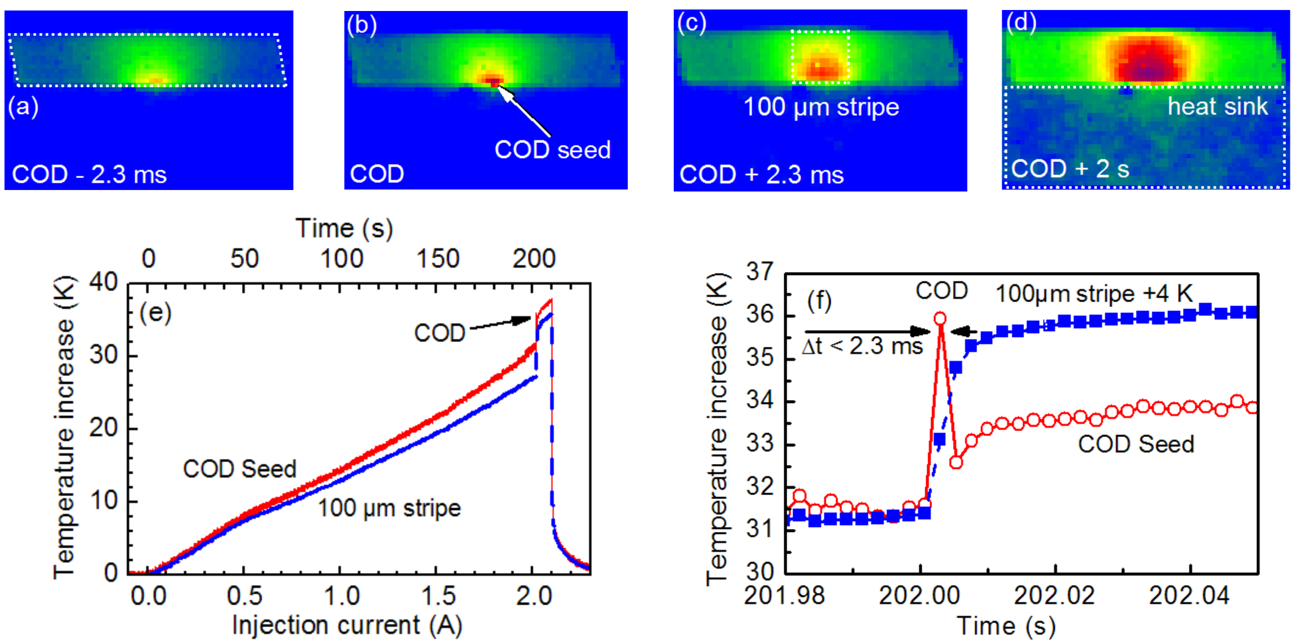

Fig. 3. Thermographic images of a red-emitting BA laser diode around the COD event: (a) 2.3 ms (i.e., one camera frame) before the COD event (outer device dimensions are marked by white dotted lines); (b) at COD, exhibiting a single camera pixel COD seed, marked by an arrow with an overshoot in the signal lasting for only this particular camera frame; (c) 2.3 ms after the COD event; (d) 2 s after the COD event where the active stripe area [marked by white dotted lines in (c)] displays an increased signal magnitude. (e,f) Temperature increase vs. time and injection current relative to the situation without current as derived from a series of images. Dashed lines and full squares correspond to average values for the 100 µm active stripe shown in (c); full lines and open circles correspond to the COD seed marked in (b). The COD event is marked by an arrow and is displayed on an expanded scale in (f).

Starting at zero current, the bulk temperature of the laser chip rises linearly up to the laser threshold at ~ 0.48 A. Above threshold, the linear slope is reduced due to stimulated emission. At the current step from 2.02 to 2.04 A, the COD takes place. In the transients of Fig. 3 (e) this is manifested as a jump in temperature by 5-8 K. Figure 3 (f) shows the transients of Fig. 3 (e) for this event at a higher temporal resolution. The red curve for the COD seed corresponds to a single pixel of the thermal images and exhibits an exceptional short temperature spike not exceeding one camera frame (2.3 ms). At the same time a rapid increase of the average bulk temperature of the stripe [Figs. 3 (c,d)] is observed. For three investigated devices the catastrophic process takes place at around 2.0-2.2 A. In order to separate the explicit dependence on the particular heat sink, the transients around the COD event are displayed in Fig. 4 after subtraction of the submount temperature, which has been measured by TI in parallel. The temperature spikes for the three unaged devices are approximately 4.0 K, 1.4 K, and 1.7 K. The slight difference between the characteristics of the laser diode in Fig. 4 (a) to the one shown in (b,c) is most probably because the devices originate from two different epitaxial runs with otherwise unchanged epitaxy. Apparently, the thermo-temporal COD characteristic is batch-dependent. This ability to resolve those slight differences can be regarded as a feature of time-resolved TI that could help us gain deeper insights into the COD-determining parameters and provide the key to even better protection against COD. Nevertheless, the very small range of critical 'COD-inducing' injection currents between 2.0 and 2.2 A indicates that local device non-uniformities play a minor role for the current values at which COD occurs.

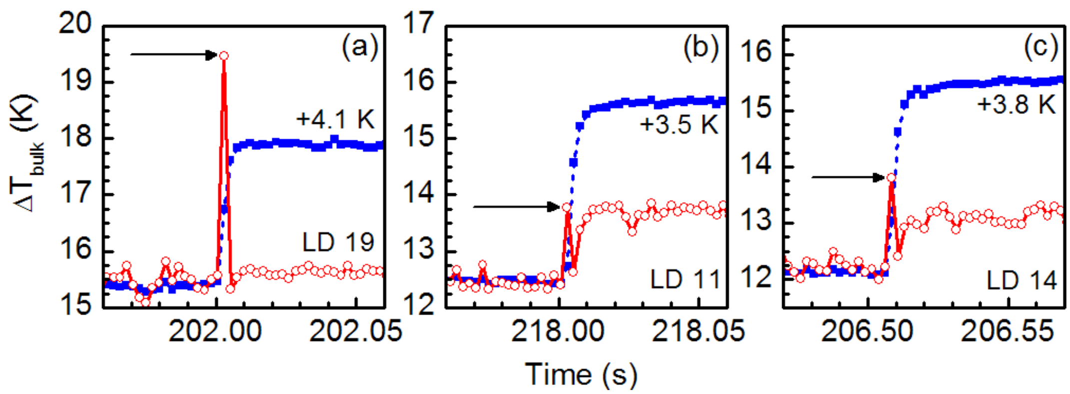

Fig. 4. Temperature increases of three laser diodes around the COD event. Symbols and lines mark the same probing areas as in Fig. 3 (f) but here the heat-sink temperature as derived from the area marked by white dotted lines in Fig. 3 (d) has been subtracted from the temperature increase. (a) corresponds to Figs. 3, (b) and (c) are measured from two devices of another batch, both with very similar COD behavior.

Due to the restrictions in spatial and temporal resolution, the COD is basically seen as a single pixel (8.8×8.8 μm^2) and single frame (2.3 ms) event. Destructive in-depth analyses[10] show COD driven defect complexes extending in vertical direction (i.e., direction of epitaxial growth) to roughly about 50-200 nm. Consequently, the derived temperature increase during the COD is only an averaged value and the true temperature increase is expected much higher. Actually, an extrapolation of the nonlinear camera-response-vs-temperature curve according to a theoretical calibration shows compatibility of the measured data with locally melting semiconductor materials at temperatures as high as ~ 1500 K.

As outlined in the preceding section, even at low currents and in early stages of degradation (under regular operation conditions) the temperature at the laser facet is (slightly) higher than in the bulk. This can be attributed to surface recombination and subsequent additional absorption. Re-absorption of the fundamental laser emission at the front facet is the most important facet heating mechanism at elevated injection currents and is proportional to the NF intensity distribution.

Thus the NF should be the key to understanding the COD at high-power operation. It should be noted, that facet temperatures derived from μR scanning of similar red-emitting devices showed indeed a close, nearly linear relation with the optical NF.[28] In Fig. 5 we show an evolution of the NF with injection current. Two regions at around the center of each half of the device show filaments with a rather high intensity. There the highest facet temperatures are expected as well. The comparison between Figs. 5 (b) and (c), i.e., between lateral profiles taken from thermal images and the corresponding NF distributions, does indeed demonstrate that the temperature spike (COD seed) occurs at the same point in space as the strongest peak of the NF distribution. This peak is reached in the NF camera frame just before COD, and followed by a nearly complete decline of the emission.

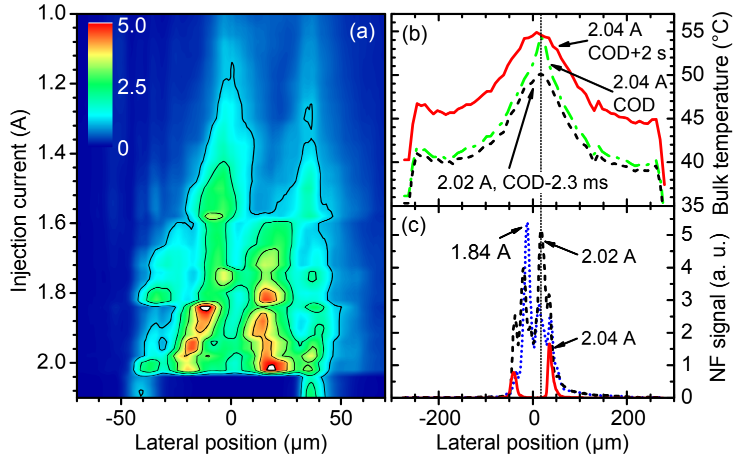

Fig. 5. (a) NF intensity vs. injection current. COD occurred between 2.02 and 2.04 A. Equipotential lines at intensities of 1, 2, 3, 4, and 5 a.u. are given. (b) Absolute bulk temperature profiles along a line that contains the active region. Corresponding NF profiles before and after COD [black and red lines as in (a)]. The dotted (blue) line represents the highest NF intensity observed at I=1.84 A.

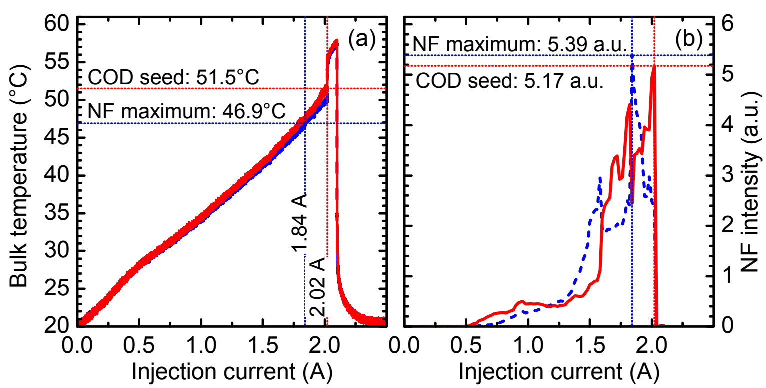

Fig. 6. Temperature and NF characteristics vs. injection current for two points at the active region of the laser diode of Figs. 3 and 5, namely the COD seed at a lateral position at around 19 µm (full lines) and the point of highest NF intensity at around -12 µm (dashed lines). (a) Absolute bulk temperature (b) NF intensity. Dotted horizontal and vertical lines mark the two prominent situations: (i) highest ever observed NF intensity at I=1.84 A with bulk temperature of 46.9°C, Intensity ~5.39 a.u., (ii) the situation just before the COD event at I=2.02 A with bulk temperature of 51.5°C, Intensity ~5.17 a.u.

The combination of the two imaging methods strongly suggests that the COD process in high-power AlGaInP laser diodes is indeed triggered by a thermal runaway process at the front facet. In this framework, the high optical facet load due to re-absorption of red laser light leads to a local melting of the semiconductor materials. Fed by the optical field, this molten site propagates along the resonator. The experimentally observed temperature spike is compatible with such a local melting. After successive re-crystallization a dense network of defects is left behind, leading to a vastly increased non-radiative recombination rate, which experimentally is found as the pronounced jump in the average device temperature.

From this concerted approach the concept of a COD critical temperature becomes evident. A closer inspection of the data shown in Fig. 5 (a) shows that the intensity of the NF filament observed at the left device side at 1.84 A was already higher than the one that actually lead to the COD at 2.04 A. A direct comparison of the two parameters bulk temperature and NF intensity, see Fig. 6, shows that only the combination of a high optical load at the facet plus a high thermal load in the bulk leads to the COD. Since both processes contribute to the facet heating, a critical facet temperature and a high photon flux can be regarded as the key precondition for the occurrence of COD. Similarly, earlier experiments on analogous devices showed that the injection-current level leading to COD falls with increasing heat-sink temperature.

Figure 6 allows for an estimate of the critical facet temperature. Assuming an additive linear relation between facet temperature T_{facet}, bulk temperature T_{bulk}, and NF intensity I_{NF}, $T_{\text{facet}} = T_{\text{bulk}} + a \times I_{\text{NF}}$ the data yield a maximal numerical value for the constant a ~21 K/a.u. Thus a maximal facet temperature of about 160°C is reached ~2 s before initiation of the actual COD process that then takes place within an interval of 2.3 ms. This number corresponds well with values on the order of 100-200°C derived from Raman spectroscopic measurements under operation conditions with power levels of about 90 percent of the COD power.[28]

SUMMARY

The microscopic processes accompanying the COD process at the front facets of semiconductor lasers are discussed in line with recent experiments. Two aspects are considered: first, the role of surface recombination as an origin of facet heating and a source of gradual degradation at any operation condition. These are preconditions and early stages towards the COD. Second, the fast COD process has been spatially and temporally resolved.

For 808 and 650 nm edge-emitting BA devices, relevant parameters such as surface recombination velocities, bulk and front facet temperatures are determined using two-color TR PL, TI, and µR spectroscopy, respectively. We find surface recombination velocities in the range $<10^5$ to 10^6 cm/s for devices with tailored surface properties. In the low-power regime, we observe rising facet temperatures as surface recombination increases. For higher optical loads, re-absorption of laser light further enhances facet heating, in particular for surfaces with a higher surface recombination velocity. Facet temperature measurements as a function of the injection current demonstrate that the temperature at the laser output facet rises linearly with the optical output power, whereas facet temperature profiles across the laser stripe reveal a strong correlation between near-field intensity, COD signatures, and facet temperatures. Temperature-power analysis shows a critical facet temperature to be required for initiating the COD process. The experimental results point to absorption of stimulated photons at the laser facet to be the major source of facet heating close to the COD event.

Finally, the dynamics of the COD process are analyzed by simultaneous high-speed infrared thermal and optical imaging of the emitter stripe. The process is revealed as fast (<2.3 ms) and spatially confined (< 8.8 × 8.8 square micron). It is connected with a pronounced impulsive temperature flash detected by the thermocamera.

Further work will aim to speed-up the temporal resolution when analyzing the COD process.

ACKNOWLEGEMENT

The authors would like to thank Peter Ressel, Bernd Sumpf, and Götz Erbert of Ferdinand-Braun-Institut für Höchstfrequenztechnik for providing high-quality diode lasers. The work on the infrared-devices was supported by the German BMBF within the BRILASI project, contract 13N8601, whereas the COD-experiments with red-emitting devices are funded by the European Commission within the Integrated Project WWW.BRIGHTER.EU, contract No. 035266.

REFERENCES

[1] A. Oosenbrug and E. E. Latta, "High-Power Operational Stability of 980 nm Pump Lasers for EDFA Applications," LEOS 1994, Boston, paper DL 1.2

[2] M. Gasser and E. E. Latta, "Method for Mirror Passivation of Semiconductor Laser Diodes," U.S. Patent 5 144 634, Sep. 1, 1992.

[3] H. Li, T. Towe, I. Chyr, D. Brown, T. Nguyen, F. Reinhardt, X. R. Srinivasan, M. Berube, T. Truchan, R. Bullock, and J. Harrison "Near 1 kW of Continuous-Wave Power From a Single High-Efficiency Diode-Laser Bar," IEEE Photon. Tech. Lett. 19, 960-962 (2007).

[4] C. H. Henry, P. M. Petroff, R. A. Logan, and F. R. Meritt, "Catastrophic damage of $Al_xGa_{1-x}As$ double-heterostructure laser material" J. Appl. Phys. 50, 3721-3732 (1979).

[5] W. C. Tang and H. J. Rosen and P. Vettiger, and D. J. Webb "Raman microprobe study of the time development of AlGaAs single quantum well laser facet temperature on route to catastrophic breakdown," Appl. Phys. Lett. 58, 557-559 (1991).
[6] P. G. Eliseev, "Optical strength of semiconductor laser materials, " Prog. Quantum Electron. 20, 1-82 (1996).
[7] H. Fujii and Y. Ueno and K. Endo "Effect of thermal resistivity on the catastrophic optical damage density of AIGalnP laser diodes," Appl. Phys. Lett. 62, (17), 2114-2115 (1993).
[8] R. E. Mallard and R. Clayton "EBIC and TEM analysis of catastrophic optical damage in high power GaAlAs/GaInAs lasers," Proc. SPIE 3004, 145 (1997).
[9] C. W. Snyder and J. W. Lee and R. Hull and R. A. Logan "Catastrophic degradation lines at the facet of InGaAsP/InP lasers investigated by transmission electron microscopy," Appl. Phys. Lett. 67, 488-490, (1995).
[10] M. Bou Sanayeh, A. Jaeger, W. Schmid, S. Tautz, P. Brick, K. Streubel, and G. Bacher "Investigation of dark line defects induced by catastrophic optical damage in broad-area AlGaInP laser diodes," Appl. Phys. Lett. 89, 101111, 1-3 (2006).
[11] K. H. Park and J. K. Lee and D. H. Jang and H. S. Cho and C. S. Park and K. E. Pyun and J. Y. Jeong and S. Nahm and J. Jeong "Characterization of catastrophic optical damage in Al-free InGaAs/InGaP 0.98 μm high-power lasers," Appl. Phys. Lett. 73, 2567-2569 (1998).
[12] T. S. Yeoh and J. A. Chaney and M. S. Leung and N. A. Ives and Z. D. Feinberg and J. G. Ho and J. Wen "Three-dimensional failure analysis of high power semiconductor laser diodes operated in vacuum," J. of Appl. Phys. 102, 123104, 1-3 (2007).
[13] S.N.G. Chu and S. Nakahara,M.E. Twigg, L.A. Koszi, E.J. Flynn, A.K. Chin, B.P. Seeger, W.D. Johnston, Jr. "Defect mechanisms in degradation of 1.32 μm wavelength channeled-substrate buried heterostructure lasers," J. Appl. Phys. 63, 611 (1988).
[14] M. Levinshtein, S. Rumyantsev, and M. Shur, [Handbook series on semiconductor parameters], World Scientific Publishing Co. Pte. Ltd., Singapore (2000).
[15] F. A. Houle, D. L. Neiman, W. C. Tang, and H. J. Rosen, "Chemical changes accompanying facet degradation of AlGaAs quantum well lasers," J. Appl. Phys. 72, 3884-3896 (1992).
[16] A. Chavan, R. Radionova, G.W. Charache, R.J. Menna, H. Schluter, J.L. Hostetler, "Comparison of facet temperature and degradation of unpumped and passivated facets of Al-free 940-nm lasers using photoluminescence," IEEE J. Quant. Electr. 41, 630-635 (2005).
[17] A. Jakubowicz "Material and fabrication-related limitations to high-power operation of GaAs/AlGaAs and InGaAs/AlGaAs laser diodes," Mater. Sci. Eng. B 44, 359-363 (1997).
[18] J. Jimenez, "Laser diode reliability: crystal defects and degradation modes," C. R. Physique 4, 663-673 (2003)..
[19] M. Fukuda and K. Takahei, "Optically enhanced oxidation of III-V compound semiconductors," J. Appl. Phys. 57, 129-134 (1985).
[20] T. Schoedl, U.T. Schwarz, V. Kümmler, M. Furitsch, A. Leber, A. Miler, A. Lell, and V. Härle, "Facet degradation of GaN heterostructure laser diodes," J. Appl. Phys. 97, 123102, 1-3 (2005).
[21] S. M. Sze, [Physics of Semiconductor Devices], 2nd ed. Wiley, New York, 51 (1981).
[22] V. Malyarchuk, J. W. Tomm, V. Talalaev, Ch. Lienau, F. Rinner, and M. Baeumler "Nanoscopic measurements of surface recombination velocity and diffusion length in a semiconductor quantum well," Appl. Phys. Lett. 81 346-348 (2002).
[23] Mathias Ziegler, Vadim Talalaev, Jens W. Tomm, Thomas Elsaesser, Peter Ressel, Bernd Sumpf, and Götz Erbert, "Surface recombination and facet heating in high-power diode lasers," Appl. Phys. Lett. 92, 203506, 1-3 (2008).
[24] V. G. Talalaev, J. W. Tomm, N. D. Zakharov, P. Werner, U. Gösele, B. V. Novikov, A. S. Sokolov, Y. B. Samsonenko, V. A. Egorov, and G. E. Cirlin, "Transient carrier transfer in tunnel injection structures," Appl. Phys. Lett. 93, 031105, 1-3 (2008).
[25] R. K. Ahrenkiel, Current Topics in Photovoltaics 3, 1 (1988).
[26] R. K. Ahrenkiel, "Minority-Carrier Lifetime in III-V Semiconductors", Semiconductors and Semimetals 39, Academic Press, Inc., 39-150, (1993).
[27] Mathias Ziegler, Jens W. Tomm, Thomas Elsaesser, Clemens Matthiesen, Marwan Bou Sanayeh, and Peter Brick; "Real-time thermal imaging of catastrophic optical damage in red-emitting high-power diode lasers," Appl. Phys. Lett. 92, 103514, 1-3 (2008).
[28] M. Bou Sanayeha, P. Brick, W. Schmid, B. Mayer, M. Müller, M. Reufer, K. Streubel J. W. Tomm, and G. Bacher "Temperature-power dependence of catastrophic optical damage in AlGaInP laser diodes," Appl. Phys. Lett. 91, 041115, 1-3 (2007).